Thermodynamic Uncertainty Relation in Interacting Many-Body Systems

Timur Koyuk and Udo Seifert*
II. Institut für Theoretische Physik, Universität Stuttgart, 70550 Stuttgart, Germany

(Received 16 February 2022; revised 1 June 2022; accepted 6 October 2022; published 17 November 2022)

The thermodynamic uncertainty relation (TUR) has been well studied for systems with few degrees of freedom. While, in principle, the TUR holds for more complex systems with many interacting degrees of freedom as well, little is known so far about its behavior in such systems. We analyze the TUR in the thermodynamic limit for mixtures of driven particles with short-range interactions. Our main result is an explicit expression for the optimal estimate of the total entropy production in terms of single-particle currents and correlations between two-particle currents. Quantitative results for various versions of a driven lattice gas demonstrate the practical implementation of this approach.

DOI: 10.1103/PhysRevLett.129.210603

Introduction.—Fluctuating currents and their correlations are a characteristic signature of stationary nonequilibrium systems. Exact results like the fluctuation theorem [1–5] and the Harada-Sasa relation [6] represent prominent, universal predictions that relate currents and their correlations to the arguably most central quantity for such systems: the rate of entropy production. More recently, the thermodynamic uncertainty relation (TUR) [7–9] has revealed an unexpected constraint on the precision of any current in terms of the total entropy production rate. Being a trade-off relation between precision and thermodynamic cost, in the sense that a high precision requires a large amount of entropy production, the TUR provides valuable insights into small mesoscopic nonequilibrium systems. It has opened a variety of promising applications for molecular motors [10], heat engines [11–15], optimal design principles for self-assembly [16], or constraints on time windows in anomalously diffusing systems [17]. From the perspective of thermodynamic inference, being a simple tool for estimating entropy production by measuring experimentally accessible currents and their fluctuations without knowing interaction potentials or driving forces, the TUR has been established as an indispensable and complementary addition to more sophisticated inference methods [18–21].

To explore these two key properties of the TUR in more complex situations, subsequent work has focused on extending its range of applicability to a variety of systems, including the observation of steady states in finite times [22,23], underdamped dynamics [24–31], stochastic field theories [32], observables that are even under time-reversal [33–35], first-passage times [36,37], relaxation processes [38–40], periodically [41,42], and arbitrary time-dependently driven systems [43,44]. Several of these generalizations have been (re)derived by using virtual perturbations or information theoretic bounds [38,45]. Last but not least, various studies have worked on generalizations of the TUR to open quantum systems [46–56].

When dealing with generalizations and refinements of the TUR, a crucial question is how sharp the corresponding bounds typically are. Early analyses showed that the TUR can be saturated in the linear response regime due to Gaussian fluctuations [7,8,57,58]. More recent studies have revealed that for the same reason it can become tight in the short-time limit [59,60]. The same situation has been observed for the time-dependent TUR in the fast-driving limit [44,61]. In all these cases, only the current of total entropy production, or a current proportional to it, leads to an equality in the TUR. Further works have focused on finding the optimal observable(s) leading to the tightest possible bound [58,60,62–67]. More specifically, using a sum of two observables and, thus, using correlations between them, can yield a sharper bound [68].

Most of the specific studies so far have treated single-particle systems or systems with a few degrees of freedom on a mesoscopic scale with a notable exception of Ref. [69]. As a crucial refinement of the TUR, the multidimensional thermodynamic uncertainty relation (MTUR) [70] should become useful when dealing with multiple currents and their correlations. While this refinement provides, in principle, the possibility of analyzing systems with many interacting degrees of freedom, a systematic study of the thermodynamic limit is still missing.

In this Letter, we analyze the TUR in the thermodynamic limit and derive the optimal estimate of entropy production using the MTUR. Our results hold for any driven many-particle system obeying a Markovian dynamics on a discrete set of states or overdamped Langevin equations for which the overall current and its variance scale as the system size and the correlation between two tagged particles decays like the inverse one. We will illustrate our theoretical predictions with various versions of a driven lattice gas.

TUR in many-particle systems.—The thermodynamic uncertainty relation has been proven under quite general conditions for both continuous-time Markov processes and systems obeying coupled overdamped Langevin equations. It is valid for any current and reads [7–9]

$$\sigma_{\rm est}^{J} \equiv J^2/D_J \leq \sigma, \tag{1}$$

where J is the mean current, $D_J \equiv \mathcal{T}\mathrm{Var}[J]/2$ is its diffusion coefficient, and $\mathcal{T}$ denotes the observation time. The precision J^2/D_J bounds the total entropy production rate σ and, hence, yields an operationally accessible estimate $\sigma_{\rm est}^{J}$ for it. To analyze the sharpness of the TUR, we define the quality factor as $\mathcal{Q}_J \equiv \sigma_{\rm est}^{J}/\sigma > 0$, which is 1 if the TUR is saturated. Since the TUR, Eq. (1), holds for any current in the system, we can use an arbitrary linear combination of currents to build the estimate $\sigma_{\rm est}^{J}$.

To study the TUR of interacting many-particle systems, we use a refinement of the TUR—the so-called MTUR introduced in Ref. [70]. We consider a system that consists of N driven interacting particles leading to N linearly independent time-averaged particle currents $\{J^{(i)}\}$. The MTUR can be applied by inserting the optimal linear combination of these currents into Eq. (1). Within this class of currents, it thus yields the sharpest lower bound on the entropy production, which is given by

$$\sigma_{\rm est}^{\boldsymbol{J}} \equiv \boldsymbol{J}^T \boldsymbol{\mathcal{C}}^{-1} \boldsymbol{J} \leq \sigma. \tag{2}$$

The estimator $\sigma_{\rm est}^{\boldsymbol{J}}$ involves the vector of particle currents $\boldsymbol{J} \equiv [J^{(1)}, \ldots, J^{(N)}]$ and the inverse of the symmetric correlation matrix $\boldsymbol{\mathcal{C}}$ with elements

$$\mathcal{C}_{ij} \equiv D^{(i)}\delta_{i,j} + C^{(ij)}(1-\delta_{i,j}). \tag{3}$$

The diagonal element $D^{(i)} \equiv \mathcal{T}\mathrm{Var}[J^{(i)}]/2$ is the diffusion coefficient of the current $J^{(i)}$ of the ith particle and the off-diagonal elements $C^{(ij)} \equiv \mathcal{T}\mathrm{Cov}[J^{(i)}, J^{(j)}]/2$ are the scaled covariances between the currents $J^{(i)}$ and $J^{(j)}$ (see Eqs. (A10) and (A11), respectively, in Appendix A).

We use the MTUR to obtain the optimal estimate for entropy production in the thermodynamic limit for a system with different species of particles. In the following, we analyze homogeneous systems in a one-phase region consisting of indistinguishable particles with pairwise short-range interactions, where the external and interaction forces are identical within a species.

First, we consider a system with only one species driven by a thermodynamic force f. Because of homogeneity, the mean values $J^{(i)} \equiv J$, diffusion coefficients $D^{(i)} \equiv D$, and correlations $C^{(ij)} \equiv C$ are independent of the particle labels. Since the particles are indistinguishable, each current contributes with the same weight to the optimal linear combination such that the MTUR reduces to the ordinary TUR for the total particle current. Hence, the estimate is given by [71]

$$\sigma_{\rm est}^{\boldsymbol{J}} = \frac{NJ^2}{D - C + NC}, \tag{4}$$

while the true entropy production reads $\sigma = \beta f N J$ with the inverse temperature β and $k_B = 1$. We assume that the diffusion coefficient of the total particle current scales like N, which is the case for driven overdamped Langevin systems with pair interactions. This implies that in the thermodynamic limit $N \to \infty$, the correlations decay like $C \approx \gamma/N$ with amplitude γ. For Langevin systems, the amplitude γ is given by the difference in the bare diffusion constant and the self-diffusion constant of a tagged particle in the interacting system (for details, see Appendix B).

When taking the thermodynamic limit $N \to \infty$, the quality factor becomes

$$\mathcal{Q}_{\boldsymbol{J}} \equiv \frac{\sigma_{\rm est}^{\boldsymbol{J}}}{\sigma} = \frac{J^\infty}{\beta f (D^\infty + \gamma)}, \tag{5}$$

where J^∞ and D^∞ are the values of the current and the self-diffusion coefficient of a tagged particle, respectively, in the thermodynamic limit. Equation (5) is our first main result and shows that the quality of the estimate depends solely on quantities related to one or two tagged particles.

Next, we study a homogeneous system consisting of a mixture of N_1 particles of species 1 and N_2 particles of species 2. The first and second species are driven by forces f_1 and f_2, respectively. Particles interact with a short-range interaction, which may be different between the species. The mean particle currents within a species are identical, i.e., $J^{(i)} = J_{\alpha_i}$, where $\alpha_i \in \{1,2\}$ denotes the species of the ith particle. Analogously, the diffusion coefficients $D^{(i)} = D_{\alpha_i}$ and correlations $C^{(ij)} = C_{\alpha_i \alpha_j}$ depend only on the particle species. Using Eq. (2) we get the estimate [71]

$$\sigma_{\rm est}^{\boldsymbol{J}} = \frac{\eta_2 N_1 J_1^2 + \eta_1 N_2 J_2^2 - 2N_1 N_2 J_1 J_2 C_{12}}{\eta_1 \eta_2 - N_1 N_2 C_{12}^2}, \tag{6}$$

with $\eta_\alpha \equiv D_\alpha + (N_\alpha - 1)C_{\alpha\alpha}$ and $\alpha \in \{1,2\}$. The true entropy production is given by $\sigma = \beta f_1 N_1 J_1 + \beta f_2 N_2 J_2$. When taking the thermodynamic limit $N = N_1 + N_2 \to \infty$, we keep the densities $\rho_\alpha \equiv N_\alpha/N$ fixed. Analogously to the one-species case, we expect that the correlations $C_{11} \approx \gamma_1/N$, $C_{22} \approx \gamma_2/N$, and $C_{12} \approx \gamma_{12}/N$ decay proportionally to the inverse system size with correlation amplitudes γ_1, γ_2, and γ_{12} (see Appendix B). Thus, the quality factor in the thermodynamic limit reads

$$\mathcal{Q}_{\boldsymbol{J}} = \frac{\eta_2^\infty \rho_1 (J_1^\infty)^2 + \eta_1^\infty \rho_2 (J_2^\infty)^2 - 2J_1^\infty J_2^\infty \rho_1 \rho_2 \gamma_{12}}{[\eta_1^\infty \eta_2^\infty - \rho_1 \rho_2 \gamma_{12}^2]\beta(f_1 \rho_1 J_1^\infty + f_2 \rho_2 J_2^\infty)}, \tag{7}$$

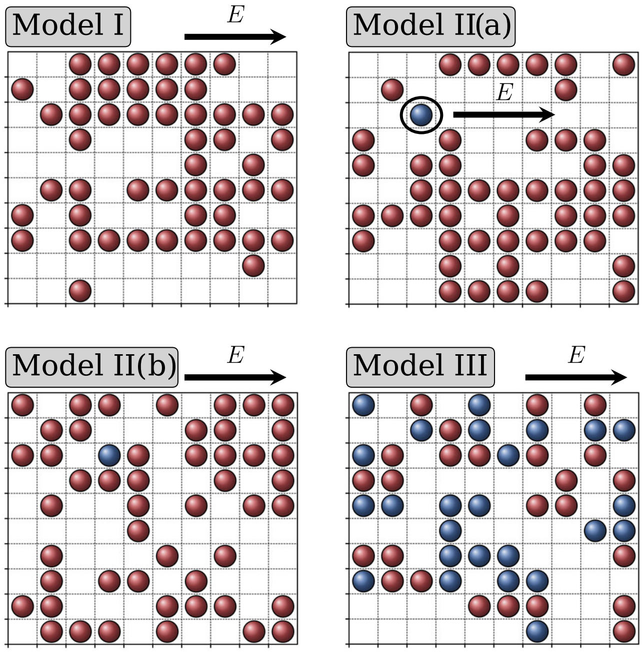

FIG. 1. Three different models of the driven lattice gas I–III. In model II(a) there is only one particle (the blue one) driven by the electric field, whereas in model II(b) all particles are driven.

where $\eta_\alpha^\infty \equiv D_\alpha^\infty + \rho_\alpha \gamma_\alpha$ and $J_{1,2}^\infty$ and $D_{1,2}^\infty$ denote the values of the currents and diffusion coefficients in this limit, respectively. The quality factor in Eq. (7) is our second main result. In contrast to the one-species case, this quality factor differs from the quality factor obtained by using as a current the total power [71]. In both cases, the MTUR remains a useful tool to infer entropy production, which, in particular, does not require the knowledge of any thermodynamic forces, as we will now illustrate for the driven lattice gas.

Driven lattice gas.—We consider a driven lattice gas [72] in which N charged particles occupy sites on a periodic $(L \times L)$–square lattice subject to an exclusion interaction as shown in Fig. 1. The particles are driven by an electric field applied in the x direction. Moreover, each particle interacts with its nearest neighbors either repulsively or attractively. The occupation variable $n_i(\boldsymbol{r}) \equiv \delta_{\boldsymbol{r}_i,\boldsymbol{r}}$ at position $\boldsymbol{r} \equiv (x, y)$ is 1, if particle i at $\boldsymbol{r}_i \equiv (x_i, y_i)$ occupies this site and is zero, otherwise. The configuration of the system is denoted by $\Gamma \equiv \{n_i(\boldsymbol{r})\}$, which contains information about all particle positions $R_\Gamma \equiv \{\boldsymbol{r}_1, \ldots, \boldsymbol{r}_N\}$.

In the following, we consider a system consisting of two species of particles with different charges q_1 and q_2. The interaction energy of the total system is given by

$$E_{\text{int}}(\Gamma) \equiv -\sum_{i>j} K_{\alpha_i\alpha_j} \sum_{\langle \boldsymbol{r}\boldsymbol{r}'\rangle} n_i(\boldsymbol{r}) n_j(\boldsymbol{r}'), \qquad (8)$$

where $\sum_{\langle \boldsymbol{r}\boldsymbol{r}'\rangle}$ denotes a summation over all nearest-neighbor-site pairs and $K_{\alpha_i\alpha_j}$ is the coupling constant of species α_i and α_j with $\alpha_{i,j} \in \{1, 2\}$. If $K_{\alpha_i\alpha_j} > 0$ the interaction is attractive; otherwise it is repulsive. The probability $p(\Gamma, t)$ to find the system in configuration Γ at time t obeys the master equation

$$\partial_t p(\Gamma, t) = \sum_{\substack{\boldsymbol{r}_i \in R_\Gamma, \\ \boldsymbol{r}'_i \in \mathcal{N}(\boldsymbol{r}_i)}} [p(\Gamma^{\boldsymbol{r}_i\boldsymbol{r}'_i}, t) k(\boldsymbol{r}'_i, \boldsymbol{r}_i, \Gamma^{\boldsymbol{r}_i\boldsymbol{r}'_i}) - p(\Gamma, t) k(\boldsymbol{r}_i, \boldsymbol{r}'_i, \Gamma)], \qquad (9)$$

where $\mathcal{N}(\boldsymbol{r}_i)$ denotes a set of all unoccupied nearest-neighbor sites $\boldsymbol{r}'_i \equiv (x'_i, y'_i)$ of position $\boldsymbol{r}_i$ and $\Gamma^{\boldsymbol{r}_i\boldsymbol{r}'_i}$ denotes a configuration identical to Γ except that particle i occupies $\boldsymbol{r}'_i$ instead of $\boldsymbol{r}_i$. The transition rate for a particle at $\boldsymbol{r}_i$ to move to an unoccupied nearest-neighbor site $\boldsymbol{r}'_i$ fulfills the local detailed balance condition and is given by

$$k(\boldsymbol{r}_i, \boldsymbol{r}'_i, \Gamma) \equiv \begin{cases} k_0 \exp(-\beta\kappa\Delta F), & \Delta F \geq 0 \\ k_0 \exp(\beta[1-\kappa]\Delta F), & \Delta F < 0 \end{cases}, \qquad (10)$$

with

$$\Delta F \equiv E_{\text{int}}(\Gamma) - E_{\text{int}}(\Gamma^{\boldsymbol{r}_i\boldsymbol{r}'_i}) + (x_i - x'_i) q_{\alpha_i} E. \qquad (11)$$

The rate amplitude k_0 sets the timescale for a transition, $q_{\alpha_i} \in \{q_1, q_2\}$ denotes the charge of the moving particle, and the parameter κ determines the rate splitting.

Quality factors.—We now analyze three paradigmatic models as depicted in Fig. 1. Model I consists of a single-particle species with density 1/2, which has been introduced in Ref. [72]. In Model II, there are N_1 particles of species 1 (red) and one single particle of species 2 (blue). Here, we distinguish two subclasses of models, which we denote as II(a) and II(b). In Model II(a) only the single particle of species 2 is charged, i.e., $q_1 = 0$ and $q_2 \neq 0$, whereas in Model II(b) all particles are charged with, in general, $q_1 \neq q_2$. The number of particles of the first species is chosen such that the density is 1/2. Model II(a) corresponds to, e.g., a driven particle in a colloidal suspension. Model III consists of two species (red and blue particles) with different charges, interactions, and densities $\rho_1 = \rho_2 = 1/4$. This model describes a binary mixture of driven particles. Similar models have been analyzed in, e.g., Refs. [73,74]. For all models, we fix the parameters $k_0 = 0.5$, $\beta = 1.0$, $E = 1.0$, and $\kappa = 1.0$ and choose an attractive interaction, i.e., $K_{11}, K_{22}, K_{12} > 0$. Moreover, we choose an observation time of $\mathcal{T} = 1000.0$ to sample trajectories by using the Gillespie algorithm [75]. In the following, we analyze these systems for different system sizes $L \times L$ and an overall density of 1/2.

Figure 2(a) shows the single-particle currents J_1 and J_2 of the two species for the models II(a) and II(b). The single driven particle in model II(a) generates a particle current J_1 of the N_1 nondriven particles by pushing or pulling them in

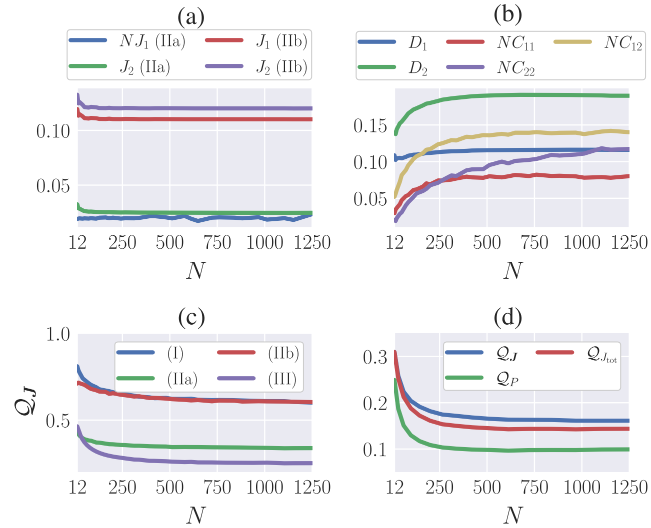

FIG. 2. (a) Particle currents of models II(a) and II(b), (b) diffusion coefficients and correlations of model III, (c) quality factors of all models against N, and (d) different quality factors $\mathcal{Q}_J$, $\mathcal{Q}_\sigma$, and $\mathcal{Q}_{J_{\rm tot}}$ for model III. For model I, $q_1 = 1.0$ and $K_{11} = 0.8$. For models II(a) and II(b), $q_1 = 0$, $q_2 = 1.0$, $K_{11} = 0.8$, and $K_{12} = 1.2$ and $q_1 = 1.0$, $q_2 = 2.5$, $K_{11} = 0.8$, and $K_{12} = 1.2$, respectively. For model III in (c), $q_1 = 1.0$, $q_2 = 2.5$, $K_{11} = 0.8$, $K_{12} = 1.2$, and $K_{22} = 0.4$, whereas in (d) $q_1 = 1.5$, $q_2 = 5.0$, $K_{11} = 0.8$, $K_{12} = 1.2$, and $K_{22} = 0.4$.

the x direction through the exclusion interaction and an attractive short-range interaction. Since this push and pull mechanism is a local effect, the number of pushed or pulled particles saturates in the thermodynamic limit, whereas the system size grows linearly in N. As a consequence, the current J_1 vanishes like $1/N$, whereas the current J_2 of the driven particle is finite as shown in Fig. 2(a). The optimal estimate of entropy production can be obtained by setting $N_2 = 1$ and $C_{22} = 0$ in Eq. (6) since there is only one particle of the second species. The true entropy production is given by $\sigma = \beta q_2 E J_2$. Combined with the fact that $J_1 \sim 1/N$ vanishes, these results imply that, in the thermodynamic limit $N \to \infty$, the quality factor becomes the quality factor of a single-particle problem $\mathcal{Q}_J = J_2^\infty/(\beta q_2 E D_2^\infty)$. The correlations between the particles do not contribute to the quality factor in contrast to model I with one single species [cf. Eq. (5)].

In model II(b), both particle currents $J_{1,2}$ are finite in the thermodynamic limit as shown in Fig. 2(a). The quality factor can analogously be obtained by setting formally $N_2 = 1$ and $C_{22} = 0$ in Eq. (6) and using $\sigma = \beta N_1 q_1 E J_1 + \beta q_2 E J_2$. When taking the thermodynamic limit $N = N_1 + 1 \to \infty$, only quantities of the first species contribute such that the quality factor reduces to the quality factor of a single interacting species of particles, i.e., $\mathcal{Q}_J = J_1/(\beta q_1 E[D_1 + \gamma_{11}])$. Therefore, the quality factors of the one-species system (a) and of system II(b) converge to the same value for $N \to \infty$ as illustrated in Fig. 2(c), which shows the quality factors for the different models I–III.

In model III, the diffusion coefficients D_1 and D_2 of the two species converge to finite values as shown in Fig. 2(b). In the accessible region of parameters, the correlations C_{11}, C_{22}, and C_{12} decay like $1/N$ since the product with the number of particles converges to a finite value as shown in Fig. 2(b). Thus, in this range of accessible system sizes, we see no signature of logarithmic corrections (yet) predicted by the corresponding field theory [76]. Furthermore, for a small number of particles $N \lesssim 12$, model III becomes similar to model II(a): in both models, species 1 is either not driven or more weakly driven in contrast to species 2, which is strongly driven. This explains why the quality factors of both models in Fig. 2(c) approach each other for small N. However, for large N model II(a) is effectively a single-particle problem and differs substantially from model III, in which many driven particles interact. Thus, the quality factor reaches the larger value $\mathcal{Q}_J \simeq 0.38$ for model II(b), whereas it reaches $\mathcal{Q}_J \simeq 0.30$ for model III. Most importantly, even though all quality factors shown in Fig. 2(c) decrease monotonically in N, they approach a finite value of order 1 for large N. In this limit, model III has the smallest quality factor since the particles are driven more strongly due to larger charges. Stronger driving leads to a smaller quality factor since the particle currents and their fluctuations saturate for large driving due to the exclusion interaction [72] while the entropy production increases.

Inference of entropy production.—We finally compare different estimates of the entropy production for the most interesting model III. The optimal quality factor $\mathcal{Q}_J$ obtained from the MTUR, Eq. (2), the quality factor using the total power as a current $\mathcal{Q}_P$, and the quality factor $\mathcal{Q}_{J_{\rm tot}}$ of the total particle current $J_{\rm tot} \equiv N_1 J_1 + N_1 J_2$ are plotted against N in Fig. 2(d). As expected, the quality factor $\mathcal{Q}_J$ beats the other two. The quality factor based on the power is even smaller than $\mathcal{Q}_{J_{\rm tot}}$ and reaches a finite value of order 1. This is quite remarkable since it shows that the additional knowledge of thermodynamic forces entering the power does not yield a better estimate. A situation related to ours has been discussed in Ref. [63], where the authors have optimized a state-dependent increment for a current and found that the best estimate does not coincide with the total entropy production. In contrast to their approach, we use constant increments and build the optimal linear combination of currents via the MTUR.

Conclusion.—In this Letter, we have analyzed the thermodynamic uncertainty relation for interacting many-particle systems in the thermodynamic limit. We have calculated the quality factor using the MTUR for homogeneous systems consisting of a single species of particles and for mixtures of two species. As we have shown, the TUR remains a useful tool for inferring entropy production since, crucially, the quality factors approach a finite order of 1 in the thermodynamic limit. From an operational perspective, it is not necessary to know the driving fields or the interactions between the particles in order to deduce the optimal estimate for entropy production. For a given number of particles, it suffices to measure the currents and correlations between two tagged ones. Although these correlations vanish with increasing system size, they are crucial ingredients of our main results in Eqs. (4)–(7) that depend on the interactions and forces of the underlying model. Even for a one-component system like the driven lattice gas, these correlations are nontrivial and are not analytically accessible. However, they are operationally accessible through trajectory data and, hence, enable one to obtain an estimator for entropy production.

To summarize, by showing that the TUR can be applied, and how it can be applied, to interacting many-body systems, we have laid the foundation for future works analyzing the TUR under various perspectives. For instance, an interesting next issue is to study how the TUR can be applied to more complex setups, e.g., in systems with different phases or at a phase transition aiming at thermodynamic inference. We further stress that our results apply to continuous overdamped Langevin systems as well. For such systems, analyzing the TUR for different interaction potentials or for systems with more than two species is a further important next step to explore macroscopic effects of the TUR. Since our tools rely on a widely applicable mathematical framework, our results should open the way for future research to study the thermodynamic limit of generalizations of the TUR, e.g., for time-dependently driven systems or for open quantum systems.

Appendix A: Definition of currents.—We define the currents entering the TUR and the MTUR in Eqs. (1) and (2), respectively. Since these two relations are valid for discrete and continuous systems, we define currents for both system types. For the sake of simplicity, we consider two-dimensional systems. We first define currents for a general two-dimensional overdamped Langevin equation and then for the driven lattice gas as an example for a system with a discrete set of states.

We consider N particles in two dimensions at positions $\boldsymbol{r} \equiv (\boldsymbol{r}_1, \ldots, \boldsymbol{r}_N)$ with coordinates $\boldsymbol{r}_i \equiv (x_i, y_i)$ obeying the overdamped Langevin equation

$$\partial_t \boldsymbol{r}_t \equiv \dot{\boldsymbol{r}}_t = \boldsymbol{\mu}[-\nabla V_{\mathrm{int}}(\boldsymbol{r}_t) + \boldsymbol{f}] + \sqrt{2}\mathbf{G}\boldsymbol{\zeta}_t. \tag{A1}$$

Here, $\boldsymbol{\mu}$ is the $2N \times 2N$ mobility matrix, $\nabla V_{\mathrm{int}}(\boldsymbol{r}_t)$ is the gradient of a short-range pair-interaction potential that depends on the distance between two labeled particles, $\boldsymbol{f} \equiv [\boldsymbol{f}^{(1)}, \ldots, \boldsymbol{f}^{(N)}]$ is a vector containing N nonconservative forces $\boldsymbol{f}^{(i)} \equiv [f_x{}^{(i)}, f_y{}^{(i)}]$ with spatial components $f_x{}^{(i)}$ and $f_y{}^{(i)}$, $\mathbf{G}$ is a $2N \times 2N$ matrix used to define the symmetric diffusion matrix $\mathbf{D} \equiv \mathbf{G}\mathbf{G}^T = \boldsymbol{\mu}/\beta$, and $\boldsymbol{\zeta}_t \equiv [\boldsymbol{\zeta}_t^{(1)}, \ldots, \boldsymbol{\zeta}_t^{(N)}]$ is a vector of N white Gaussian noises $\boldsymbol{\zeta}_t^{(i)} \equiv [\zeta_x{}^{(i)}(t), \zeta_y{}^{(i)}(t)]$ describing the random forces with mean $\langle \zeta_x{}^{(i)}(t) \rangle = 0$ and correlations $\langle \zeta_a{}^{(i)}(t)\zeta_b{}^{(j)}(t') \rangle = \delta_{a,b}\delta_{ij}\delta(t-t')$, where $a, b \in \{x, y\}$. A general fluctuating current along the trajectory $\boldsymbol{r}_t$ of length $\mathcal{T}$ reads

$$J[\boldsymbol{r}_t] \equiv \frac{1}{\mathcal{T}} \int_0^{\mathcal{T}} dt \boldsymbol{d}(\boldsymbol{r}_t) \circ \dot{\boldsymbol{r}}_t, \tag{A2}$$

where $\boldsymbol{d}(\boldsymbol{r}_t) \equiv [\boldsymbol{d}^{(1)}(\boldsymbol{r}_t), \ldots, \boldsymbol{d}^{(N)}(\boldsymbol{r}_t)]$ is a vector of arbitrary increments $\boldsymbol{d}^{(i)}(\boldsymbol{r}_t) \equiv [d_x^{(i)}(\boldsymbol{r}_t), d_y^{(i)}(\boldsymbol{r}_t)]$ and $\circ$ denotes the Stratonovich product. The choice $\boldsymbol{d}(\boldsymbol{r}) = \beta \boldsymbol{f}$ in Eq. (A2) corresponds to the total power

$$P[\boldsymbol{r}_t] \equiv \frac{1}{\mathcal{T}} \int_0^{\mathcal{T}} dt \beta \boldsymbol{f} \circ \dot{\boldsymbol{r}}_t. \tag{A3}$$

Choosing $\boldsymbol{d}(\boldsymbol{r}) = \boldsymbol{e}_x^{(i)}$ as the unit vector of particle i in direction x, we get the current in x direction of particle i as

$$J^{(i)}[\boldsymbol{r}_t] \equiv \frac{1}{\mathcal{T}} \int_0^{\mathcal{T}} dt \dot{x}_i(t) \tag{A4}$$

with mean value $J^{(i)} \equiv \langle J^{(i)}[\boldsymbol{r}_t] \rangle$.

Next, we consider currents for the driven lattice gas. The fluctuating current of particle i along the trajectory Γ_t of length $\mathcal{T}$ reads

$$J^{(i)}[\Gamma_t] \equiv \frac{1}{\mathcal{T}} [n_{x^+}^{(i)}(\mathcal{T}) - n_{x^-}^{(i)}(\mathcal{T})], \tag{A5}$$

where $n_{x^+}^{(i)}(\mathcal{T})$ and $n_{x^-}^{(i)}(\mathcal{T})$ denote the total number of jumps of particle i in positive and in negative x direction up to time $\mathcal{T}$, respectively. The mean value in Eq. (A5) is defined as $J^{(i)} \equiv \langle J^{(i)}[\Gamma_t] \rangle$. Using Eq. (A5), we define the particle currents of species 1 and 2 as

$$J_1[\Gamma_t] \equiv \frac{1}{N_1} \sum_{i=1}^{N} \delta_{1,\alpha_i} J^{(i)}[\Gamma_t] \tag{A6}$$

and

$$J_2[\Gamma_t] \equiv \frac{1}{N_2} \sum_{i=1}^{N} \delta_{2,\alpha_i} J^{(i)}[\Gamma_t], \tag{A7}$$

respectively. We denote the corresponding mean values by $J_1 \equiv \langle J_1[\Gamma_t] \rangle$ and $J_2 \equiv \langle J_2[\Gamma_t] \rangle$. The total power is given by

$$P[\Gamma_t] \equiv \beta q_1 E N_1 J_1[\Gamma_t] + \beta q_2 E N_2 J_2[\Gamma_t] \tag{A8}$$

with mean value $P \equiv \langle P[\Gamma_t] \rangle = \beta q_1 E N_1 J_1 + \beta q_2 E N_2 J_2$. The total particle current reads

$$J_{\text{tot}}[\Gamma_t] \equiv \sum_{i=1}^{N} J^{(i)}[\Gamma_t] \tag{A9}$$

with mean value $J_{\text{tot}} \equiv \langle J_{\text{tot}}[\Gamma_t] \rangle = N_1 J_1 + N_2 J_2$.

For currents in both, continuous and discrete systems, the diffusion coefficient and the correlations between two particle currents are defined as

$$D^{(i)} = \mathcal{T}\text{Var}[J^{(i)}]/2 \equiv \mathcal{T}\langle (J^{(i)}[X_t] - J^{(i)})^2 \rangle/2 \tag{A10}$$

and

$$C^{(ij)} = \mathcal{T}\text{Cov}[J^{(i)}, J^{(j)}]/2 \equiv \mathcal{T}(\langle J^{(i)}[X_t] J^{(j)}[X_t] \rangle - J^{(i)} J^{(j)})/2, \tag{A11}$$

respectively, with $X_t \in \{\boldsymbol{r}_t, \Gamma_t\}$. The mean values of the power in Eqs. (A3) and (A8) coincide with the mean total entropy production, i.e., $\sigma \equiv \langle P[X_t] \rangle$. However, for any finite time $\mathcal{T}$, their fluctuating values and consequently their diffusion coefficients are different. In contrast, for long observation times $\mathcal{T} \to \infty$, the total fluctuating power becomes the total entropy production, i.e., $P[X_t] \approx \sigma[X_t]$, as the contribution of the change in internal energy and in stochastic entropy vanishes asymptotically.

Appendix B: Generic scaling of correlations.—We discuss the scaling of the correlations in the thermodynamic limit. Our analysis is based on the assumption that the diffusion coefficient of the total particle current scales like N. First, we prove that this condition is always satisfied for the general Langevin dynamics defined in Eq. (A1). Then, we show that the correlations can be expected to decay like $1/N$ for continuous and discrete systems if this basic assumption holds true.

As outlined above, the necessary condition for the $1/N$ scaling of the correlations is that the diffusion coefficient of the total particle current scales with the system size. We first prove this property for overdamped Langevin systems with two species obeying Eq. (A1), where each particle has the same mobility. A proof for an arbitrary number of species or for particles with a different mobility is straightforward. In the latter case, it suffices to prove the N scaling for the diffusion coefficient of a current that is a linear combination of currents of a tagged particle as we will show in the next section.

We consider an overdamped Langevin system of two species of particles with different nonconservative forces and interactions. We assume that all particles have the same mobility μ and bare diffusion constant $\tilde{D} = \mu/\beta$. The Langevin equation of the ith particle reads

$$\dot{\boldsymbol{r}}_i(t) = \mu \boldsymbol{f}^{(i)} + \mu \sum_{j \neq i} \boldsymbol{F}_{\boldsymbol{r}_i}^{(ij)}(|\boldsymbol{r}_i(t) - \boldsymbol{r}_j(t)|) + \sqrt{2\tilde{D}} \boldsymbol{\zeta}_t^{(i)} \tag{B1}$$

with the interaction force $\boldsymbol{F}_{\boldsymbol{r}_i}^{(ij)}(|\boldsymbol{r}_i(t) - \boldsymbol{r}_j(t)|) \equiv -\nabla_{\boldsymbol{r}_i} V_{\text{int}}^{(ij)}(|\boldsymbol{r}_i - \boldsymbol{r}_j|)|_{\boldsymbol{r}_{i,j} = \boldsymbol{r}_{i,j}(t)}$, $\nabla_{\boldsymbol{r}_i} \equiv (\partial_{x_i}, \partial_{y_i})$, and $V_{\text{int}}^{(ij)}(|\boldsymbol{r}_i - \boldsymbol{r}_j|)$ an arbitrary interaction potential between particle i and j. For the sake of simplicity, we assume $\boldsymbol{f}^{(i)} = (f_x^{(i)}, 0)$, i.e., the particles are driven into the x direction. Then, the particle current in Eq. (A4) is given by

$$J^{(i)}[\boldsymbol{r}_t] = \frac{1}{\mathcal{T}} \int_0^{\mathcal{T}} dt \left[\mu f_x^{(i)} + \mu \sum_{j \neq i} F_{x_i}^{(ij)}(|\boldsymbol{r}_i(t) - \boldsymbol{r}_j(t)|) + \sqrt{2\tilde{D}} \zeta_x^{(i)}(t) \right] \tag{B2}$$

with the interaction force $F_{x_i}^{(ij)}(|\boldsymbol{r}_i(t) - \boldsymbol{r}_j(t)|) \equiv -\partial_{x_i} V_{\text{int}}^{(ij)}(|\boldsymbol{r}_i - \boldsymbol{r}_j|)|_{\boldsymbol{r}_{i,j} = \boldsymbol{r}_{i,j}(t)}$. Summing over all particles in Eq. (B2) yields the total particle current

$$J_{\text{tot}}[\boldsymbol{r}_t] = \frac{1}{\mathcal{T}} \int_0^{\mathcal{T}} dt \left[\mu N_1 f_1 + \mu N_2 f_2 + \sqrt{2\tilde{D}} \sum_{i=1}^{N} \zeta_x^{(i)}(t) \right] \tag{B3}$$

with forces f_1 and f_2 acting on species 1 and 2, respectively. Here, we have used that $\sum_{i,j,i \neq j} \partial_{x_i} V_{\text{int}}^{(ij)}(|\boldsymbol{r}_i - \boldsymbol{r}_j|) = 0$, i.e., the sum over all interaction forces vanishes. Since the random forces acting on two different particles are uncorrelated, the diffusion coefficient of the current in Eq. (B3) is given by $D_{J_{\text{tot}}} = N\tilde{D}$ and, hence, it scales linearly with the system size. The scaling holds also for more than two species since the nonconservative forces do not fluctuate. Furthermore, for particles with a different mobility one could construct the current

$$J^{\dagger}[\boldsymbol{r}_t] \equiv \sum_{i=1}^{N} J^{(i)}[\boldsymbol{r}_t]/\mu^{(i)} = \sum_{i=1}^{N} \left(f_x^{(i)} + \frac{1}{\mathcal{T}} \int_0^{\mathcal{T}} \mathrm{d}t \, \zeta_t^{(i)}/\beta \right) \tag{B4}$$

that does not coincide with the total particle current. However, its diffusion coefficient $D_{J^{\dagger}} = N/\beta$ scales with system size as well. We will need this current below.

We first discuss the scaling of correlation functions in the single species case, where we assume that the diffusion coefficient of the total particle current scales like N. Using Eq. (20) in Ref. [71] with $\Phi_1 = 1$ and $\Phi_2 = 0$ leads to $D_{J_{\text{tot}}} = ND + N(N-1)C$. Assuming that $D_{J_{\text{tot}}} = ND_0$ with D_0 a constant of order 1 and that the self-diffusion coefficient of a tagged particle D is of order 1, we get the condition $C = (D_0 - D)/(N-1)$ for the correlations.

This relation shows that the correlations decay like $1/N$ in the thermodynamic limit. For an overdamped Langevin system with a single species, D_0 coincides with the bare diffusion constant $\tilde{D}$. Thus, for these systems, we get $\gamma = \tilde{D} - D$, i.e., the correlation amplitude is given by the difference between the bare diffusion constant and the self-diffusion coefficient of a tagged particle.

For the two species case, we get from Eq. (20) in Ref. [71] with $\Phi_1 = \Phi_2 = 1$

$$D_{J_{\mathrm{tot}}} = N_1 D_1 + N_2 D_2 + N_1(N_1 - 1)C_{11} + N_2(N_2 - 1)C_{22} + 2N_1 N_2 C_{12}. \quad \text{(B5)}$$

Assuming that the diffusion coefficient scales like $D_{J_{\mathrm{tot}}} = N D_0$ with a constant D_0 leads to the following condition:

$$(D_0 - \rho_1 D_1 - \rho_2 D_2) = N(\rho_1^2 C_{11} + \rho_2^2 C_{22} + 2\rho_1\rho_2 C_{12}) - \rho_1 C_{11} - \rho_2 C_{22}. \quad \text{(B6)}$$

Under the assumption of vanishing correlations and single-particle diffusion coefficients of order 1 in the thermodynamic limit, we get

$$(\rho_1^2 C_{11} + \rho_2^2 C_{22} + 2\rho_1\rho_2 C_{12}) = \frac{(D_0 - \rho_1 D_1 - \rho_2 D_2)}{N} \quad \text{(B7)}$$

for large N. We note that for overdamped two-species Langevin systems, D_0 is the bare diffusion coefficient $\tilde{D}$. Equation (B7) shows that the sum of all correlation functions must decay like $1/N$ in thermodynamic limit.

For $N \to \infty$, there are two scenarios, in principle. First, each correlation function decays like $C_{11} \approx \gamma_1/N$, $C_{22} \approx \gamma_2/N$, and $C_{12} \approx \gamma_{12}/N$. In analogy with the single species case, we expect this to be the generic case. Second, the correlation functions could scale like $1/N$ plus a term that decays slower than $1/N$. In this case, the amplitudes of the latter terms must cancel in Eq. (B7) since the right-hand side scales with $1/N$. We note that in the latter case, the quality factor of the total particle current is of order 1. Therefore, the quality factor using the MTUR must also be of order 1 and cannot vanish in the thermodynamic limit.

Finally, we note that for overdamped Langevin systems, where the particles have a different mobility, we can use the current introduced in Eq. (B4) to follow the steps from above and choose the increments in Eq. (20) in Ref. [71] as a species-dependent mobility. In this case, we get a similar condition to Eq. (B7) with additional factors of the species-dependent mobility. Since these factors are model-dependent constants, they do not affect the scaling in N and, thus, the discussion from above applies similarly.

*Correspond author.
useifert@theo2.physik.uni-stuttgart.de

[1] D. J. Evans, E. G. D. Cohen, and G. P. Morriss, Probability of Second Law Violations in Shearing Steady States, Phys. Rev. Lett. **71**, 2401 (1993).
[2] G. Gallavotti and E. G. D. Cohen, Dynamical Ensembles in Nonequilibrium Statistical Mechanics, Phys. Rev. Lett. **74**, 2694 (1995).
[3] J. Kurchan, Fluctuation theorem for stochastic dynamics, J. Phys. A **31**, 3719 (1998).
[4] J. L. Lebowitz and H. Spohn, A Gallavotti-Cohen-type symmetry in the large deviation functional for stochastic dynamics, J. Stat. Phys. **95**, 333 (1999).
[5] D. Andrieux and P. Gaspard, Fluctuation theorem for currents and Schnakenberg network theory, J. Stat. Phys. **127**, 107 (2007).
[6] T. Harada and S. I. Sasa, Equality Connecting Energy Dissipation with a Violation of the Fluctuation-Response Relation, Phys. Rev. Lett. **95**, 130602 (2005).
[7] Andre C. Barato and Udo Seifert, Thermodynamic Uncertainty Relation for Biomolecular Processes, Phys. Rev. Lett. **114**, 158101 (2015).
[8] Todd R. Gingrich, Jordan M. Horowitz, Nikolay Perunov, and Jeremy L. England, Dissipation Bounds all Steady-State Current Fluctuations, Phys. Rev. Lett. **116**, 120601 (2016).
[9] Jordan M. Horowitz and Todd R. Gingrich, Thermodynamic uncertainty relations constrain non-equilibrium fluctuations, Nat. Phys. **16**, 15 (2020).
[10] Patrick Pietzonka, Andre C Barato, and Udo Seifert, Universal bound on the efficiency of molecular motors, J. Stat. Mech. (2016) 124004.
[11] Naoto Shiraishi, Keiji Saito, and Hal Tasaki, Universal Trade-Off Relation Between Power and Efficiency for Heat Engines, Phys. Rev. Lett. **117**, 190601 (2016).
[12] Patrick Pietzonka and Udo Seifert, Universal Trade-Off Between Power, Efficiency and Constancy in Steady-State Heat Engines, Phys. Rev. Lett. **120**, 190602 (2018).
[13] Viktor Holubec and Artem Ryabov, Cycling Tames Power Fluctuations near Optimum Efficiency, Phys. Rev. Lett. **121**, 120601 (2018).
[14] Timothy Ekeh, Michael E. Cates, and Étienne Fodor, Thermodynamic cycles with active matter, Phys. Rev. E **102**, 010101(R) (2020).
[15] Giuliano Benenti, Giulio Casati, and Jiao Wang, Power, efficiency, and fluctuations in steady-state heat engines, Phys. Rev. E **102**, 040103(R) (2020).
[16] Michael Nguyen and Suriyanarayanan Vaikuntanathan, Design principles for nonequilibrium self-assembly, Proc. Natl. Acad. Sci. U.S.A. **113**, 14231 (2016).
[17] D. Hartich and A. Godec, Thermodynamic Uncertainty Relation Bounds the Extent of Anomalous Diffusion, Phys. Rev. Lett. **127**, 080601 (2021).
[18] David B. Brückner, Pierre Ronceray, and Chase P. Broedersz, Inferring the Dynamics of Underdamped Stochastic Systems, Phys. Rev. Lett. **125**, 058103 (2020).
[19] Anna Frishman and Pierre Ronceray, Learning Force Fields from Stochastic Trajectories, Phys. Rev. X **10**, 021009 (2020).

[20] Dominic J. Skinner and Jörn Dunkel, Improved bounds on entropy production in living systems, Proc. Natl. Acad. Sci. U.S.A. **118**, e2024300118 (2021).

[21] Dominic J. Skinner and Jörn Dunkel, Estimating Entropy Production from Waiting Time Distributions, Phys. Rev. Lett. **127**, 198101 (2021).

[22] Patrick Pietzonka, Felix Ritort, and Udo Seifert, Finite-time generalization of the thermodynamic uncertainty relation, Phys. Rev. E **96**, 012101 (2017).

[23] Jordan M. Horowitz and Todd R. Gingrich, Proof of the finite-time thermodynamic uncertainty relation for steady-state currents, Phys. Rev. E **96**, 020103(R) (2017).

[24] Andreas Dechant and Shin Ichi Sasa, Entropic bounds on currents in Langevin systems, Phys. Rev. E **97**, 062101 (2018).

[25] H.-M. Chun, L. P. Fischer, and U. Seifert, Effect of a magnetic field on the thermodynamic uncertainty relation, Phys. Rev. E **99**, 042128 (2019).

[26] Lukas P. Fischer, Hyun-Myung Chun, and Udo Seifert, Free diffusion bounds the precision of currents in underdamped dynamics, Phys. Rev. E **102**, 012120 (2020).

[27] Jae Sung Lee, Jong-Min Park, and Hyunggyu Park, Thermodynamic uncertainty relation for underdamped Langevin systems driven by a velocity-dependent force, Phys. Rev. E **100**, 062132 (2019).

[28] Tan Van Vu and Yoshihiko Hasegawa, Uncertainty relations for underdamped Langevin dynamics, Phys. Rev. E **100**, 032130 (2019).

[29] Jae Sung Lee, Jong-Min Park, and Hyunggyu Park, Universal form of thermodynamic uncertainty relation for Langevin dynamics, Phys. Rev. E **104**, L052102 (2021).

[30] Chulan Kwon and Hyun Keun Lee, Thermodynamic uncertainty relation for underdamped dynamics driven by time-dependent protocols, New J. Phys. **24**, 013029 (2022).

[31] Patrick Pietzonka, Classical Pendulum Clocks Break the Thermodynamic Uncertainty Relation, Phys. Rev. Lett. **128**, 130606 (2022).

[32] O. Niggemann and U. Seifert, The two scaling regimes of the thermodynamic uncertainty relation for the KPZ-equation, J. Stat. Phys. **186**, 3 (2022).

[33] Christian Maes, Frenetic Bounds on the Entropy Production, Phys. Rev. Lett. **119**, 160601 (2017).

[34] Cesare Nardini and Hugo Touchette, Process interpretation of current entropic bounds, Eur. Phys. J. B **91**, 16 (2018).

[35] I. Terlizzi and M. Baiesi, Kinetic uncertainty relation, J. Phys. A **52**, 02LT03 (2019).

[36] Todd R. Gingrich and Jordan M. Horowitz, Fundamental Bounds on First Passage Time Fluctuations for Currents, Phys. Rev. Lett. **119**, 170601 (2017).

[37] Juan P. Garrahan, Simple bounds on fluctuations and uncertainty relations for first-passage times of counting observables, Phys. Rev. E **95**, 032134 (2017).

[38] Andreas Dechant and Shin Ichi Sasa, Fluctuation–response inequality out of equilibrium, Proc. Natl. Acad. Sci. U.S.A. **117**, 6430 (2020).

[39] K. Liu, Z. Gong, and M. Ueda, Thermodynamic Uncertainty Relation for Arbitrary Initial States, Phys. Rev. Lett. **125**, 140602 (2020).

[40] David H. Wolpert, Uncertainty Relations and Fluctuation Theorems for Bayes Nets, Phys. Rev. Lett. **125**, 200602 (2020).

[41] Andre C. Barato, Raphael Chetrite, Alessandra Faggionato, and Davide Gabrielli, Bounds on current fluctuations in periodically driven systems, New J. Phys. **20**, 103023 (2018).

[42] Timur Koyuk and Udo Seifert, Operationally Accessible Bounds on Fuctuations and Entropy Production in Periodically Driven Systems, Phys. Rev. Lett. **122**, 230601 (2019).

[43] Tan Van Vu and Yoshihiko Hasegawa, Thermodynamic uncertainty relations under arbitrary control protocols, Phys. Rev. Res. **2**, 013060 (2020).

[44] Timur Koyuk and Udo Seifert, Thermodynamic Uncertainty Relation for Time-Dependent Driving, Phys. Rev. Lett. **125**, 260604 (2020).

[45] Andreas Dechant and Shin Ichi Sasa, Current fluctuations and transport efficiency for general Langevin systems, J. Stat. Mech. (2018) 063209.

[46] Katarzyna Macieszczak, Kay Brandner, and Juan P. Garrahan, Unified Thermodynamic Uncertainty Relations in Linear Response, Phys. Rev. Lett. **121**, 130601 (2018).

[47] B. K. Agarwalla and D. Segal, Assessing the validity of the thermodynamic uncertainty relation in quantum systems, Phys. Rev. B **98**, 155438 (2018).

[48] K. Ptaszyński, Coherence-enhanced constancy of a quantum thermoelectric generator, Phys. Rev. B **98**, 085425 (2018).

[49] Kay Brandner, Taro Hanazato, and Keiji Saito, Thermodynamic Bounds on Precision in Ballistic Multiterminal Transport, Phys. Rev. Lett. **120**, 090601 (2018).

[50] M. Carrega, M. Sassetti, and U. Weiss, Optimal work-to-work conversion of a nonlinear quantum Brownian duet, Phys. Rev. A **99**, 062111 (2019).

[51] G. Guarnieri, G. T. Landi, S. R. Clark, and J. Goold, Thermodynamics of precision in quantum non equilibrium steady states, Phys. Rev. Res. **1**, 033021 (2019).

[52] Federico Carollo, Robert L. Jack, and Juan P Garrahan, Unraveling the Large Deviation Statistics of Markovian Open Quantum Systems, Phys. Rev. Lett. **122**, 130605 (2019).

[53] Soham Pal, Sushant Saryal, Dvira Segal, T. S. Mahesh, and Bijay Kumar Agarwalla, Experimental study of the thermodynamic uncertainty relation, Phys. Rev. Res. **2**, 022044(R) (2020).

[54] Hava Meira Friedman, Bijay Kumar Agarwalla, Ofir Shein-Lumbroso, Oren Tal, and Dvira Segal, Thermodynamic uncertainty relation in atomic-scale quantum conductors, Phys. Rev. B **101**, 195423 (2020).

[55] Yoshihiko Hasegawa, Thermodynamic Uncertainty Relation for General Open Quantum Systems, Phys. Rev. Lett. **126**, 010602 (2021).

[56] H. J. D. Miller, M. H. Mohammady, M. Perarnau-Llobet, and G. Guarnieri, Thermodynamic Uncertainty Relation in Slowly Driven Quantum Heat Engines, Phys. Rev. Lett. **126**, 210603 (2021).

[57] Patrick Pietzonka, Andre C. Barato, and Udo Seifert, Universal bounds on current fluctuations, Phys. Rev. E **93**, 052145 (2016).

[58] Todd R Gingrich, Grant M Rotskoff, and Jordan M Horowitz, Inferring dissipation from current fluctuations, J. Phys. A **50**, 184004 (2017).

[59] Shun Otsubo, Sosuke Ito, Andreas Dechant, and Takahiro Sagawa, Estimating entropy production by machine learning of short-time fluctuating currents, Phys. Rev. E **101**, 062106 (2020).

[60] Sreekanth K. Manikandan, Deepak Gupta, and Supriya Krishnamurthy, Inferring Entropy Production from Short Experiments, Phys. Rev. Lett. **124**, 120603 (2020).

[61] Timur Koyuk and Udo Seifert, Quality of the thermodynamic uncertainty relation for fast and slow driving, J. Phys. A **54**, 414005 (2021).

[62] Matteo Polettini, Alexandre Lazarescu, and Massimiliano Esposito, Tightening the uncertainty principle for stochastic currents, Phys. Rev. E **94**, 052104 (2016).

[63] Daniel Maria Busiello and Simone Pigolotti, Hyperaccurate currents in stochastic thermodynamics, Phys. Rev. E **100**, 060102(R) (2019).

[64] Junang Li, Jordan M. Horowitz, Todd R. Gingrich, and Nikta Fakhri, Quantifying dissipation using fluctuating currents, Nat. Commun. **10**, 1666 (2019).

[65] Gianmaria Falasco, Massimiliano Esposito, and Jean-Charles Delvenne, Unifying thermodynamic uncertainty relations, New J. Phys. **22**, 053046 (2020).

[66] Tan Van Vu, Van Tuan Vo, and Yoshihiko Hasegawa, Entropy production estimation with optimal current, Phys. Rev. E **101**, 042138 (2020).

[67] Naoto Shiraishi, Optimal thermodynamic uncertainty relation in Markov jump processes, J. Stat. Phys. **185**, 19 (2021).

[68] Andreas Dechant and Shin Ichi Sasa, Improving Thermodynamic Bounds using Correlations, Phys. Rev. X **11**, 041061 (2021).

[69] Ohad Shpielberg and Arnab Pal, Thermodynamic uncertainty relations for many-body systems with fast jump rates and large occupancies, Phys. Rev. E **104**, 064141 (2021).

[70] Andreas Dechant, Multidimensional thermodynamic uncertainty relations, J. Phys. A **52**, 035001 (2019).

[71] See Supplemental Material at http://link.aps.org/supplemental/10.1103/PhysRevLett.129.210603 for the full derivations of the main results and for discussions about inference of entropy production from currents in a subvolume.

[72] S. Katz, J. L. Lebowitz, and H. Spohn, Nonequilibrium steady states of stochastic lattice gas models of fast ionic conductors, J. Stat. Phys. **34**, 497 (1984).

[73] B Schmittmann, K Hwang, and R. K. P Zia, Onset of spatial structures in biased diffusion of two species, Europhys. Lett. **19**, 19 (1992).

[74] Honghao Yu, Kristian Thijssen, and Robert L. Jack, Perpendicular and parallel phase separation in two-species driven diffusive lattice gases, Phys. Rev. E **106**, 024129 (2022).

[75] D. T. Gillespie, Exact stochastic simulation of coupled chemical reactions, J. Phys. Chem. **81**, 2340 (1977).

[76] Vivien Lecomte, Uwe C Täuber, and Frédéric van Wijland, Current distribution in systems with anomalous diffusion: renormalization group approach, J. Phys. A **40**, 1447 (2007).